

# CHARACTERIZATION AND COMPUTATION OF $\mathcal{H}_\infty$ NORMS FOR TIME-DELAY SYSTEMS

WIM MICHIELS AND SUAT GUMUSSOY\*

**Abstract.** We consider the characterization and computation of  $\mathcal{H}_\infty$  norms for a class of time-delay systems. It is well known that in the finite dimensional case the  $\mathcal{H}_\infty$  norm of a transfer function can be computed using the connections between the corresponding singular value curves and the imaginary axis eigenvalues of a Hamiltonian matrix, leading to the established level set methods. We show a similar connection between the transfer function of a time-delay system and the imaginary axis eigenvalues of an infinite dimensional linear operator  $\mathcal{L}_\xi$ . Based on this result, we propose a predictor-corrector algorithm for the computation of the  $\mathcal{H}_\infty$  norm. In the prediction step, a finite-dimensional approximation of the problem, induced by a spectral discretization of the operator  $\mathcal{L}_\xi$ , and an adaptation of the algorithms for finite-dimensional systems, allow to obtain an approximation of the  $\mathcal{H}_\infty$  norm of the transfer function of the time-delay system. In the next step the approximate results are corrected to the desired accuracy by solving a set of nonlinear equations which are obtained from the reformulation of the eigenvalue problem for the linear infinite-dimensional operator  $\mathcal{L}_\xi$  as a finite dimensional nonlinear eigenvalue problem. These equations can be interpreted as characterizations of peak values in the singular value plot. The effects of the discretization in the predictor step are fully characterized and the choice of the number of discretization points is discussed. The paper concludes with a numerical example and the presentation of the results of extensive benchmarking.

**1. Introduction.** In the field of robust control of linear systems stability and performance criteria are often expressed by means of  $\mathcal{H}_\infty$  norms of appropriately defined transfer functions [16]. Therefore, the availability of robust methods to compute  $\mathcal{H}_\infty$  norms is essential in a computer aided control system design.

In this article we present an approach to compute the  $\mathcal{H}_\infty$  norm of the transfer function

$$G(j\omega) = C \left( j\omega I - A_0 - \sum_{i=1}^m A_i e^{-j\omega\tau_i} \right)^{-1} B + D e^{-j\omega\tau_0}, \quad (1.1)$$

where  $A_i \in \mathbb{R}^{n \times n}$ ,  $0 \leq i \leq m$ ,  $B \in \mathbb{R}^{n \times n_u}$ ,  $C \in \mathbb{R}^{n_y \times n}$ ,  $D \in \mathbb{R}^{n_y \times n_u}$  are the system matrices, and the nonnegative numbers  $(\tau_0, \tau_1, \dots, \tau_m)$  correspond to time-delays. The  $\mathcal{H}_\infty$  norm of the transfer function (1.1) is finite if and only if the zeros of the equation

$$\det \left( \lambda I - A_0 - \sum_{i=1}^m A_i e^{-\lambda\tau_i} \right) = 0$$

are confined to the open left half complex plane. Under this condition it can be expressed as

$$\|G(j\omega)\|_{\mathcal{H}_\infty} = \sup_{\omega \geq 0} \sigma_1(G(j\omega)),$$

where  $\sigma_1(\cdot)$  denotes the largest singular value [16, 12].

The commonly used methods for computing  $\mathcal{H}_\infty$  norms and related robustness measures for systems without delay belong to the class of level set methods. They are based on the duality between the singular value plot of the transfer function and the

---

\*Department of Computer Science, Katholieke Universiteit Leuven, Belgium, (`{Wim.Michiels,Suat.Gumussoy}@cs.kuleuven.be`)

position of the spectrum of an appropriately defined Hamiltonian matrix with respect to the imaginary axis, as expressed in the following result from [2] (see also [8]):

PROPOSITION 1.1. *Let  $G_f(j\omega) = C(j\omega I - A)^{-1}B + D$ . Let  $\xi > 0$  be such that the matrix  $D^T D - \xi^2 I$  is non-singular. For  $\omega \geq 0$ , the matrix  $G_f(j\omega)$  has a singular value equal to  $\xi$  if and only if  $j\omega$  is an eigenvalue of the matrix*

$$L_\xi = \begin{bmatrix} A & -B(D^T D - \xi^2 I)^{-1} B^T \\ -C^T C + C^T D(D^T D - \xi^2 I)^{-1} D^T C & -A^T \end{bmatrix}.$$

From Proposition 1.1 we get

$$\|G_f(j\omega)\|_{\mathcal{H}_\infty} = \inf \{ \xi > \sigma_1(D) : L_\xi \text{ has no imaginary axis eigenvalues} \}.$$

This result directly leads a bisection algorithm on the parameter  $\xi$  for computing the  $\mathcal{H}_\infty$  norm of  $G_f(j\omega)$ , as outlined in [2]. Quadratically convergent algorithms based on a search in a two-parameter space  $(\omega, \xi)$  are presented in [1, 6]. A similar algorithm for computing pseudospectral abscissa for systems without delays is proposed in [7].

The approach of the paper to compute the  $\mathcal{H}_\infty$  norm of (1.1) builds on a generalization of Proposition 1.1 to time-delay systems. Due to the fact that a time-delay system is inherently infinite-dimensional [13], the singular value curves of (1.1) can no longer be related to the imaginary axis eigenvalues of a matrix but to the imaginary axis eigenvalues of an infinite-dimensional linear operator  $\mathcal{L}_\xi$ , as we shall see. This leads to a two-step approach for the computation of the  $\mathcal{H}_\infty$  norm of (1.1). In the first step (the prediction step), an approximation of the  $\mathcal{H}_\infty$  norm of (1.1) is computed based on a finite-dimensional approximation of the system, induced by a discretization of the operator  $\mathcal{L}_\xi$ . Because this operator is a derivative operator on a function space with nonlocal boundary condition, the discretization is done using a spectral method [14], well established for this type of operators, see [5] and the references therein. In the next step (the correction step) the approximation of the  $\mathcal{H}_\infty$  norm is improved up to the desired accuracy with a local method, by solving a set of nonlinear equations. These are obtained from the reformulation of the eigenvalue problem for the linear infinite-dimensional operator  $\mathcal{L}_\xi$  as a nonlinear eigenvalue problem of finite dimension.

The proposed method for computing  $\mathcal{H}_\infty$  norms has several similarities with some existing methods for computing characteristic roots of time-delay systems, although the underlying problems are totally different. First, the characteristic roots solve an infinite-dimensional linear eigenvalue problem as well as a finite-dimensional nonlinear eigenvalue problem (induced by the characteristic equation), see [13, 15]. This may also lead to a two-step approach, where approximations of the characteristic roots are obtained by discretizing the infinite-dimensional linear eigenvalue problem and solving the resulting matrix eigenvalue problem in the first place, and the approximate characteristic roots are corrected subsequently by Newton iterations on the nonlinear characteristic equation. Such a predictor-corrector scheme is implemented in the software package DDE-BIFTOOL [9]. Second, one of the common approaches to compute characteristic roots consists of discretizing the infinitesimal generator of the time-integration operator (solution operator) that generates the semi-flow of the solutions, see, e.g. the methods proposed in [3, 4]. The infinitesimal generator is also a derivative operator with nonlocal boundary conditions, to which a spectral discretization is employed in [4]. It forms the basis for the computation of characteristic roots by the package TRACE-DDE.

The structure of the article is as follows. In Section 2 Proposition 1.1 is generalized to transfer functions of the form (1.1). These connections form the theoretical basis of the paper. In Section 3 the properties of a finite-dimensional approximation based on a spectral discretization of the infinite-dimensional operator  $\mathcal{L}_\xi$  are discussed. In Section 4 the predictor-corrector algorithm is described in detail. Section 5 is devoted to the numerical examples. In Section 6 some concluding remarks are presented.

**Notations and assumptions.** The notations are as follows:

$\mathbb{C}, \mathbb{R}$ :	the field of the complex and real numbers
$\mathbb{R}_+$ :	set of nonnegative real numbers
$A^*$ :	complex conjugate transpose of the matrix $A$
$A^{-T}$ :	transpose of the inverse matrix of $A$
$\mathcal{D}(\cdot)$ :	domain of an operator
$I, I_n$ :	identity matrix of appropriate dimensions, of dimensions $n \times n$
$j$ :	imaginary identity
$\sigma_i(A)$ :	$i^{\text{th}}$ singular value of $A$ , $\sigma_1(\cdot) \geq \sigma_2(\cdot) \geq \dots$
$\lambda_i(A)$ :	$i^{\text{th}}$ eigenvalue of $A$ , $ \lambda_1(\cdot)  \geq  \lambda_2(\cdot)  \geq \dots$
$\Re(u)$ :	real part of the complex number $u$
$\Im(u)$ :	imaginary part of the complex number $u$
$\bar{u}$ :	complex conjugate of the complex number $u$
$ u $ :	modulus of the complex number $u$
$\det(A)$ :	determinant of the matrix $A$
$A \otimes B$ :	Kronecker product of matrices $A$ and $B$

Throughout the paper the following assumption is made:

ASSUMPTION 1.2.

$$\max_{0 \leq i \leq m} \tau_i = 1.$$

Note that Assumption 1.2 can be taken without any loss of generality because the variable  $\omega$  and the system matrices in (1.1) can always be re-scaled. It will allow us to significantly simplify the notations.

## 2. Theoretical basis.

**2.1. Relations with a Hamiltonian eigenvalue problem.** The following lemma extends Proposition 1.1 to time-delay systems:

LEMMA 2.1. *Let  $\xi > 0$  be such that the matrix*

$$D_\xi := D^T D - \xi^2 I$$

*is non-singular. For  $\omega \geq 0$ , the matrix  $G(j\omega)$  has a singular value equal to  $\xi$  if and only if  $\lambda = j\omega$  is a solution of the equation*

$$\det H(\lambda, \xi) = 0, \quad (2.1)$$

where

$$H(\lambda, \xi) := \lambda I - M_0 - \sum_{i=1}^m (M_i e^{-\lambda \tau_i} + M_{-i} e^{\lambda \tau_i}) - (N_1 e^{-\lambda \tau_0} + N_{-1} e^{\lambda \tau_0}), \quad (2.2)$$

with

$$\begin{aligned} M_0 &= \begin{bmatrix} A_0 & -BD_\xi^{-1}B^T \\ -C^TC + C^TDD_\xi^{-1}D^TC & -A_0^T \end{bmatrix}, \\ M_i &= \begin{bmatrix} A_i & 0 \\ 0 & 0 \end{bmatrix}, \quad M_{-i} = \begin{bmatrix} 0 & 0 \\ 0 & -A_i^T \end{bmatrix}, \quad 1 \leq i \leq N, \\ N_1 &= \begin{bmatrix} 0 & 0 \\ 0 & C^TDD_\xi^{-1}B^T \end{bmatrix}, \quad N_{-1} = \begin{bmatrix} -BD_\xi^{-1}D^TC & 0 \\ 0 & 0 \end{bmatrix}. \end{aligned}$$

**Proof.** The proof is similar to the proof of Proposition 22 in [10]. For all  $\omega \in \mathbb{R}$ , we have the relation

$$\det H(j\omega, \xi) \det D_\xi(j\omega) = \det(G^*(j\omega)G(j\omega) - \xi^2 I) \det \left( \begin{bmatrix} j\omega I - A_0 - \sum_{i=1}^m A_i e^{-j\omega\tau_i} & 0 \\ 0 & j\omega I + A_0^T + \sum_{i=1}^m A_i^T e^{j\omega\tau_i} \end{bmatrix} \right), \quad (2.3)$$

because both left and right hand side can be interpreted as expressions for the determinant of the 2-by-2 block matrix

$$\left[ \begin{array}{cc|c} j\omega I - A_0 - \sum_{i=1}^m A_i e^{-j\omega\tau_i} & 0 & -B \\ \hline C^TC & j\omega I + A_0^T + \sum_{i=1}^m A_i^T e^{j\omega\tau_i} & C^TD \\ \hline D^TC & B^T & D_\xi \end{array} \right]$$

using Schur complements. Because  $D_\xi$  is non-singular and  $G$  is stable, we get from (2.3):

$$\det(G^*(j\omega)G(j\omega) - \xi^2 I) = 0 \Leftrightarrow \det H(j\omega, \xi) = 0.$$

This is equivalent to the assertion of the theorem.  $\square$

For a fixed value of  $\xi$ , the solutions of (2.1) can be found by solving the nonlinear eigenvalue problem

$$H(\lambda, \xi) v = 0, \quad \lambda \in \mathbb{C}, \quad v \in \mathbb{C}^{2n}, \quad v \neq 0. \quad (2.4)$$

This nonlinear eigenvalue problem can be "linearized" to an infinite-dimensional linear eigenvalue problem. For this, we consider the space

$$X := \mathcal{C} \left( \left[ -\max_{0 \leq i \leq m} \tau_i, \max_{0 \leq i \leq m} \tau_i \right], \mathbb{C}^{2n} \right) = \mathcal{C}([-1, 1], \mathbb{C}^{2n}),$$

where we have taken into account Assumption 1.2. We let the operator  $\mathcal{L}_\xi$  on  $X$  be defined by:

$$\mathcal{D}(\mathcal{L}_\xi) = \left\{ \phi \in X : \phi' \in X, \quad \phi'(0) = M_0\phi(0) + \sum_{i=1}^m (M_i\phi(-\tau_i) + M_{-i}\phi(\tau_i)) \right. \\ \left. + N_1\phi(-\tau_0) + N_{-1}\phi(\tau_0) \right\}, \quad (2.5)$$

$$\mathcal{L}_\xi \phi = \phi', \quad \phi \in \mathcal{D}(\mathcal{L}_\xi). \quad (2.6)$$

The eigenvalue problem for this linear operator is defined as

$$(\lambda I - \mathcal{L}_\xi)u = 0 : \quad \lambda \in \mathbb{C}, \quad u \in X, \quad u \neq 0. \quad (2.7)$$

The eigenvalues of  $\mathcal{L}_\xi$  have a one-to-one correspondence to the eigenvalues of the nonlinear eigenvalue problem (2.4):

PROPOSITION 2.2. *Let  $H$  be defined by (2.2). Let  $\xi > 0$  be such that  $D^T D - \xi^2 I$  is nonsingular. Then we have*

$$\exists v \in \mathbb{C}^{2n}, v \neq 0 : H(\lambda, \xi)v = 0 \Leftrightarrow \exists u \in X, u \neq 0 : (\lambda I - \mathcal{L}_\xi)u = 0.$$

Furthermore, if  $(\lambda, u)$  satisfies (2.7), then  $u$  has the form

$$u(\theta) = ve^{\lambda\theta}, \theta \in [-1, 1], \quad (2.8)$$

where  $v \in \mathbb{C}^{2n}$  and  $(\lambda, v)$  satisfies (2.4). Conversely, if  $(\lambda, v)$  satisfies (2.4) then  $(\lambda, u)$  satisfies (2.7) with  $u$  given by (2.8).

**Proof.** Assume that  $\mathcal{L}_\xi u = \lambda u$ . From (2.6) we get  $u(t) = e^{\lambda t}v$ ,  $t \in [-1, 1]$ , with  $v \in \mathbb{C}^{2n}$ . Taking into account the boundary condition (2.5) we get  $H(\lambda, \xi)v = 0$ . Conversely, if  $H(\lambda, \xi)v = 0$ , then it is readily verified that  $u \equiv ve^{\lambda\theta}$ ,  $\theta \in [-1, 1]$ , belongs to  $\mathcal{D}(\mathcal{L}_\xi)$  and satisfies  $(\mathcal{L}_\xi - \lambda I)u = 0$ .  $\square$

By combining Lemma 2.1 and Proposition 2.2 we arrive at:

THEOREM 2.3. *Let  $\xi > 0$  be such that the matrix  $D^T D - \xi^2 I$  is non-singular. For  $\omega \geq 0$ , the matrix  $G(j\omega)$  has a singular value equal to  $\xi$  if and only if  $\lambda = j\omega$  is an eigenvalue of the operator  $\mathcal{L}_\xi$ , defined by (2.5) and (2.6).*

COROLLARY 2.4.

$$\|G(j\omega)\|_{\mathcal{H}_\infty} = \inf\{\xi > \sigma_1(D^T D) : \text{operator } \mathcal{L}_\xi \text{ has no imaginary axis eigenvalues}\}.$$

**2.2. Properties of the eigenvalue problem.** Although the operator  $\mathcal{L}_\xi$  generally has an infinite number of eigenvalues, the number of eigenvalues on the imaginary axis is always finite. This can be concluded from the following results:

PROPOSITION 2.5. *All eigenvalues of  $\mathcal{L}_\xi$  belong to the set*

$$\Xi := \left\{ \lambda \in \mathbb{C} : |\lambda| \leq \|M_0\| + \sum_{i=1}^m (\|M_i\|e^{-\Re\lambda\tau_i} + \|M_{-i}\|e^{\Re\lambda\tau_i}) + \|N_1\|e^{-\Re\lambda\tau_0} + \|N_{-1}\|e^{\Re\lambda\tau_0} \right\}.$$

**Proof.** From the identity  $\det H(\lambda, \xi) = 0$  we get

$$|\lambda| \leq \|M_0\| + \sum_{i=1}^m (\|M_i\| |e^{-\lambda\tau_i}| + \|M_{-i}\| |e^{\lambda\tau_i}|) + \|N_1\| |e^{-\lambda\tau_0}| + \|N_{-1}\| |e^{\lambda\tau_0}|.$$

The proposition follows.  $\square$

Note that  $\lambda$  appears in both left and right hand side of the inequality that defines the set  $\Xi$ . If one considers the elements of  $\Xi$  with a given real part, say  $\Re(\lambda) = p$ ,  $p \in \mathbb{R}$ , then the bound on their modulus  $|\lambda|$  is obtained by evaluating the right hand side for  $\Re(\lambda) = p$  (a value smaller than  $|p|$  implies the set  $\Xi$  has no intersection with the line  $\Re(\lambda) = p$ ).

COROLLARY 2.6. *For all  $c > 0$ , the number of eigenvalues of  $\mathcal{L}_\xi$  in the strip*

$$\{\lambda \in \mathbb{C} : -c < \Re(\lambda) < c\} \quad (2.9)$$

is finite.

**Proof.** Proposition 2.5 implies that the eigenvalues in the strip (2.9) can be constrained to a compact set. Because the function  $H(\cdot, \xi)$  is analytic this number is finite.  $\square$

The set of eigenvalues of  $\mathcal{L}_\xi$  is symmetric w.r.t. the imaginary axis, as expressed in the following proposition (for comparison, in the delay-free case the operator  $\mathcal{L}_\xi$  reduces to a Hamiltonian matrix):

**PROPOSITION 2.7.** *A complex number  $\lambda$  is an eigenvalue of  $\mathcal{L}_\xi$  if and only if  $-\bar{\lambda}$  is an eigenvalue of  $\mathcal{L}_\xi$ .*

**Proof.** It can be directly verified that

$$H(-\bar{\lambda}, \xi) = - \left( \left( \begin{bmatrix} 0 & -1 \\ 1 & 0 \end{bmatrix} \otimes I \right) H(\lambda, \xi) \left( \begin{bmatrix} 0 & 1 \\ -1 & 0 \end{bmatrix} \otimes I \right) \right)^*,$$

hence,

$$\det H(-\bar{\lambda}, \xi) = (\det H(\lambda, \xi))^* \quad (2.10)$$

and

$$\det H(-\bar{\lambda}, \xi) = 0 \Leftrightarrow \det H(\lambda, \xi) = 0.$$

This is equivalent to the statement to be proven.  $\square$

**2.3. Interpretation in a two parameter space.** We consider the equation

$$\det H(j\omega, \xi) = 0 \quad (2.11)$$

as the central equation, and look at its solutions in the two parameter space  $(\omega, \xi) \in \mathbb{R}_+ \times \mathbb{R}_+$ . From Lemma 2.1 and Proposition 2.2 we have the following corollary:

**THEOREM 2.8.** *Let  $\omega \geq 0$  and  $\xi \geq 0$  such that the matrix  $D_\xi$  is nonsingular. The following statements are equivalent:*

1.  $\det H(j\omega, \xi) = 0$ ;
2.  $j\omega$  is an eigenvalue of the operator  $\mathcal{L}_\xi$ ;
3.  $\xi$  is a singular value of the matrix  $G(j\omega)$ .

Graphically, the equation (2.11) defines a set of curves in the  $(\omega, \xi)$  parameter space. The intersections with horizontal lines ( $\xi$  fixed) can be found by computing the imaginary axis eigenvalues of  $\mathcal{L}_\xi$ . Similarly, the intersections with vertical lines ( $\omega$  fixed) can be found by computing the singular values of  $G(j\omega)$ . This is shown in Figure 2.1.

**3. Finite-dimensional approximation.** The numerical methods for computing  $\mathcal{H}_\infty$  norms presented in Section 4 are strongly based on Corollary 2.4. Because the operator  $\mathcal{L}_\xi$ , defined by (2.5)-(2.6), is infinite-dimensional, these algorithms will involve a discretization of this operator. In this section we outline a discretization approach and discuss its properties.

**3.1. Discretization.** Following the approach of [4, 5], we discretize the operator  $\mathcal{L}_\xi$  using a *spectral method* (see, e.g. [14]).

Given a positive integer  $N$ , we consider a mesh  $\Omega_N$  of  $2N + 1$  distinct points in the interval  $[-1, 1]$ :

$$\Omega_N = \{\theta_{N,i}, i = -N, \dots, N\}, \quad (3.1)$$

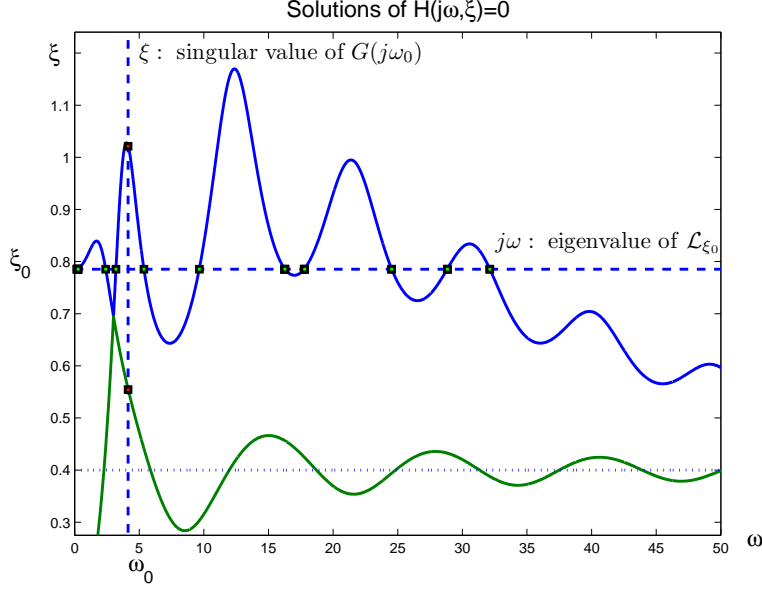


FIG. 2.1. Solutions of the equation (2.11), for the problem data (5.1).

where

$$-1 \leq \theta_{N,-N} < \dots < \theta_{N,-1} < \theta_{N,0} = 0 < \theta_{N,1} < \dots < \theta_{N,N} \leq 1$$

and

$$\theta_{N,-i} = -\theta_{N,i}, \quad i = 1, \dots, N. \quad (3.2)$$

The mesh  $\Omega_N$  allows us to replace the continuous space  $X$  with a space  $X_N$  of discrete functions. More precisely, a function  $\phi \in X$  is discretized into a block vector  $x = [x_{-N}^T \dots x_N^T]^T \in X_N$  with components

$$x_i = \phi(\theta_{N,i}) \in \mathbb{C}^{2n}, \quad i = -N, \dots, N.$$

When defining  $\mathcal{P}_N x$ ,  $x \in X_N$  as the unique  $\mathbb{C}^{2n}$  valued interpolating polynomial of degree less than or equal to  $2N$  satisfying

$$\mathcal{P}_N x(\theta_{N,i}) = x_i, \quad i = -N, \dots, N,$$

we can approximate the operator  $\mathcal{L}_\xi$  over  $X$  with the matrix  $\mathcal{L}_\xi^N : X_N \rightarrow X_N$ , defined as

$$\begin{aligned} \left( \mathcal{L}_\xi^N x \right)_i &= (\mathcal{P}_N x)'(\theta_{N,i}), & i = -N, \dots, -1, \\ \left( \mathcal{L}_\xi^N x \right)_0 &= M_0 \mathcal{P}_N x(0) + \sum_{i=1}^m (M_i \mathcal{P}_N x(-\tau_i) + M_{-i} \mathcal{P}_N x(\tau_i)) \\ &\quad + N_1 \mathcal{P}_N x(-\tau_0) + N_{-1} \mathcal{P}_N x(\tau_0), \\ \left( \mathcal{L}_\xi^N x \right)_i &= (\mathcal{P}_N x)'(\theta_{N,i}), & i = 1, \dots, N. \end{aligned} \quad (3.3)$$

An *explicit expression* for the elements of the matrix  $\mathcal{L}_\xi^N$  can be obtained by using the Lagrange representation of  $\mathcal{P}_N x$ ,

$$\mathcal{P}_N x = \sum_{k=-N}^N l_{N,k} x_k, \quad (3.4)$$

where the Lagrange polynomials  $l_{N,k}$  are real valued polynomials of degree  $2N$  satisfying

$$l_{N,k}(\theta_{N,i}) = \begin{cases} 1 & i = k, \\ 0 & i \neq k. \end{cases}$$

By substituting (3.4) in (3.3) we obtain the expression

$$\mathcal{L}_\xi^N = \begin{bmatrix} d_{-N,-N} & \dots & d_{-N,N} \\ \vdots & & \vdots \\ d_{-1,-N} & \dots & d_{-1,N} \\ a_{-N} & \dots & a_N \\ d_{1,-N} & \dots & d_{1,N} \\ \vdots & & \vdots \\ d_{N,-N} & \dots & d_{N,N} \end{bmatrix} \in \mathbb{R}^{(2N+1)(2n) \times (2N+1)2n},$$

where

$$\begin{aligned} d_{i,k} &= l'_{N,k}(\theta_{N,i})I, \quad i \in \{-N, \dots, -1, 1, \dots, N\}, \quad k \in \{-N, \dots, N\}, \\ a_0 &= M_0 + \sum_{k=1}^m (M_k l_{N,0}(-\tau_k) + M_{-k} l_{N,0}(\tau_k)) + N_1 l_{N,0}(-\tau_0) + N_{-1} l_{N,0}(\tau_0), \\ a_i &= \sum_{k=1}^m (M_k l_{N,i}(-\tau_k) + M_{-k} l_{N,i}(\tau_k)) + N_1 l_{N,i}(-\tau_0) + N_{-1} l_{N,i}(\tau_0), \\ & \quad i \in \{-N, \dots, -1, 1, \dots, N\}. \end{aligned}$$

It is important to note that all the problem specific information and the parameter  $\xi$  are concentrated in the middle row of  $\mathcal{L}_\xi^N$ , i.e. the elements  $(a_{-N}, \dots, a_N)$ , while all other elements of  $\mathcal{L}_\xi^N$  can be computed beforehand.

We outline some properties of the matrix  $\mathcal{L}_\xi^N$ . First, analogously to the continuous case the (linear) eigenvalue problem for  $\mathcal{L}_\xi^N$ ,

$$\mathcal{L}_\xi^N x = \lambda x, \quad \lambda \in \mathbb{C}, \quad x \in \mathbb{C}^{(2N+1)2n}, \quad x \neq 0, \quad (3.5)$$

has a nonlinear eigenvalue problem of dimension  $2n$  as counterpart. To clarify this we need the following definition:

**DEFINITION 3.1.** For  $\lambda \in \mathbb{C}$ , let  $p_N(\cdot; \lambda)$  be the polynomial of degree  $2N$  satisfying

$$\begin{aligned} p_N(0; \lambda) &= 1, \\ p'_N(\theta_{N,i}; \lambda) &= \lambda p_N(\theta_{N,i}; \lambda), \quad i \in \{-N, \dots, -1\} \cup \{1, \dots, N\}. \end{aligned} \quad (3.6)$$

Note that the polynomial  $p_N(t; \lambda)$  is an approximation of  $\exp(\lambda t)$  on the interval  $[-1; 1]$ . Indeed, the first equation of (3.6) is an interpolation requirement at zero, the other equations are collocation conditions for the differential equation  $\dot{z} = \lambda z$ , of which  $\exp(\lambda t)$  is a solution. We can now state:

**PROPOSITION 3.2.** *The following statements are equivalent:*

$$\exists x \in \mathbb{C}^{(2N+1)2n}, \quad x \neq 0 : (\lambda I - \mathcal{L}_\xi^N) x = 0 \Leftrightarrow \exists v \in \mathbb{C}^{2n}, \quad v \neq 0 : H_N(\lambda, \xi)v = 0,$$



where

$$H_N(\lambda, \xi) := \lambda I - M_0 - \sum_{i=1}^m (M_i p_N(-\tau_i; \lambda) + M_{-i} p_N(\tau_i; \lambda)) - (N_1 p_N(-\tau_0; \lambda) + N_{-1} p_N(\tau_0; \lambda)). \quad (3.7)$$

**Proof.** Using (3.3) the expression (3.5) can be written as:

$$(\mathcal{P}_N x)'(\theta_{N,i}) = \lambda x_i = \lambda \mathcal{P}_N x(\theta_{N,i}), \quad i \in \{-N, \dots, -1, 1, \dots, N\}, \quad (3.8)$$

$$M_0 \mathcal{P}_N x(0) + \sum_{i=1}^m (M_i \mathcal{P}_N x(-\tau_i) + M_{-i} \mathcal{P}_N x(\tau_i)) + N_1 \mathcal{P}_N x(-\tau_0) + N_{-1} \mathcal{P}_N x(\tau_0) = \lambda x_0 = \lambda \mathcal{P}_N x(0). \quad (3.9)$$

From  $\mathcal{P}_N x(0) = x_0$  and (3.8) it follows that

$$\mathcal{P}_N x(\cdot) = p_N(\cdot; \lambda) x_0. \quad (3.10)$$

When substituting (3.10) in (3.9) we arrive at  $H_N(\lambda, \xi) x_0 = 0$ .  $\square$

Notice that  $H_N(\lambda, \xi)$  can be obtained from  $H(\lambda, \xi)$ , by making the substitution

$$e^{-\lambda \tau_i} \leftarrow p_N(-\tau_i; \lambda), \quad i = -N, \dots, N.$$

As we shall see in §4.1 the functions  $p_N(-\tau_i; \lambda)$  are proper rational functions of the parameter  $\lambda$ . Thus, the effect of a spectral discretization of the operator  $\mathcal{L}_\xi$  can be interpreted as the effect of a *rational approximation* of the exponential functions in  $H(\lambda, \xi)$ .

Second, the spectral property described in Proposition 2.7 is preserved, due to the symmetry of the grid:

**PROPOSITION 3.3.** *A complex number  $\lambda$  is an eigenvalue of  $\mathcal{L}_\xi^N$  if and only if  $-\bar{\lambda}$  is an eigenvalue of  $\mathcal{L}_\xi^N$ .*

**Proof.** The property (3.2) of the grid assures that

$$p_N(-\tau_i; \lambda) = p_N(\tau_i; -\lambda), \quad \forall \lambda \in \mathbb{C}, \quad \forall i \in \{0, \dots, m\}.$$

Using this result, the similar arguments as in the proof of Proposition 2.7 lead us to

$$\det H_N(-\bar{\lambda}, \xi) = 0 \Leftrightarrow \det H_N(\lambda, \xi) = 0,$$

which is equivalent to the statement of the proposition.  $\square$

**3.2. Interpretation in a two parameter space.** Similarly as in §2.3 we characterize the solutions of the two-parameter problem

$$\det H_N(j\omega, \xi) = 0, \quad (3.11)$$

where  $\omega \geq 0$  and  $\xi \geq 0$ . The counterpart of Theorem 2.8 reads as:

**THEOREM 3.4.** *Let  $\omega \geq 0$  and let  $\xi \geq 0$  such that the matrix  $D_\xi$  is nonsingular. The following statements are equivalent:*

1.  $\det H_N(j\omega, \xi) = 0$ ;
2.  $j\omega$  is an eigenvalue of  $\mathcal{L}_\xi^N$ ;

3.  $\xi^2$  is an eigenvalue of the matrix

$$M_N(j\omega) := \begin{bmatrix} X_N(j\omega) + X_N(j\omega)^* + Y_N(j\omega)^* Y_N(j\omega) + D^T D & \sqrt{r(\omega)} X_N(j\omega)^* \\ \sqrt{r(\omega)} X_N(j\omega) & D^T D \end{bmatrix} \quad (3.12)$$

where

$$\begin{aligned} X_N &= D^T C (j\omega I - A_0 - \sum_{i=1}^m A_i p_N(-\tau_i; j\omega))^{-1} B p_N(\tau_0; j\omega), \\ Y_N &= C (j\omega I - A_0 - \sum_{i=1}^m A_i p_N(-\tau_i; j\omega))^{-1} B, \\ r_N(\omega) &= \frac{1}{|p_N(-\tau_0; j\omega)|^2} - 1. \end{aligned}$$

**Proof.** The equivalence between the first and second statement corresponds to Proposition 3.2. Therefore, it is sufficient to prove the equivalence between the first and the third statement.

We can express  $H_N(j\omega, \xi)$  as

$$H_N(j\omega, \xi) = \begin{bmatrix} j\omega I - A_0 - \sum_{i=1}^m A_i p_N(-\tau_i; j\omega) & 0 \\ C^T C & 0 \end{bmatrix} \begin{bmatrix} j\omega I + A^T + \sum_{i=1}^m A_i^T p_N(\tau_i; j\omega) \\ (D^T D - \xi^2 I)^{-1} & 0 \\ 0 & (D^T D - \xi^2 I)^{-1} \end{bmatrix} + \begin{bmatrix} B & 0 \\ 0 & -C^T D p_N(-\tau_0; j\omega) \end{bmatrix} \cdot \begin{bmatrix} p_N(\tau_0; j\omega) D^T C & B^T \\ \frac{1}{p_N(-\tau_0; j\omega)} D^T C & B^T \end{bmatrix}.$$

Since the transfer function (1.1) has no poles on the imaginary axis, we have

$$\det H_N(j\omega, \xi) = 0 \Leftrightarrow \det \tilde{H}_N(j\omega, \xi) = 0,$$

where

$$\begin{aligned} \tilde{H}_N(j\omega, \xi) &:= \xi^2 I - \begin{bmatrix} D^T D & 0 \\ 0 & D^T D \end{bmatrix} - \begin{bmatrix} p_N(\tau_0; j\omega) D^T C & B^T \\ \frac{1}{p_N(-\tau_0; j\omega)} D^T C & B^T \end{bmatrix} \\ &\quad \begin{bmatrix} j\omega I - A_0 - \sum_{i=1}^m A_i p_N(-\tau_i; j\omega) & 0 \\ C^T C & j\omega I + A^T + \sum_{i=1}^m A_i^T p_N(\tau_i; j\omega) \end{bmatrix}^{-1} \\ &\quad \cdot \begin{bmatrix} B & 0 \\ 0 & -C^T D p_N(-\tau_0; j\omega) \end{bmatrix}. \end{aligned}$$

Using an explicit formula for the inverse of a two-by-two block matrix, we obtain:

$$\tilde{H}_N(j\omega, \xi) = \xi^2 I - \begin{bmatrix} D^T D + X_N(j\omega) + Y_N(j\omega)^* Y_N(j\omega) & X_N(j\omega)^* \\ \frac{1}{|p_N(-\tau_0; j\omega)|^2} X_N(j\omega) + Y_N(j\omega)^* Y_N(j\omega) & D^T D + X_N(j\omega)^* \end{bmatrix}.$$

By elementary row and column operations we arrive at

$$\det \tilde{H}_N(j\omega, \xi) = \det (\xi^2 I - M_N(j\omega)),$$

hence,

$$\det H_N(j\omega, \xi) = 0 \Leftrightarrow \det (\xi^2 I - M_N(j\omega)) = 0.$$

This completes the proof.  $\square$

The graphical interpretation of Theorem 3.4 is as follows. The intersections between the curves in the  $(\omega, \xi)$  plane, defined by (3.11), with horizontal lines ( $\xi$  fixed)

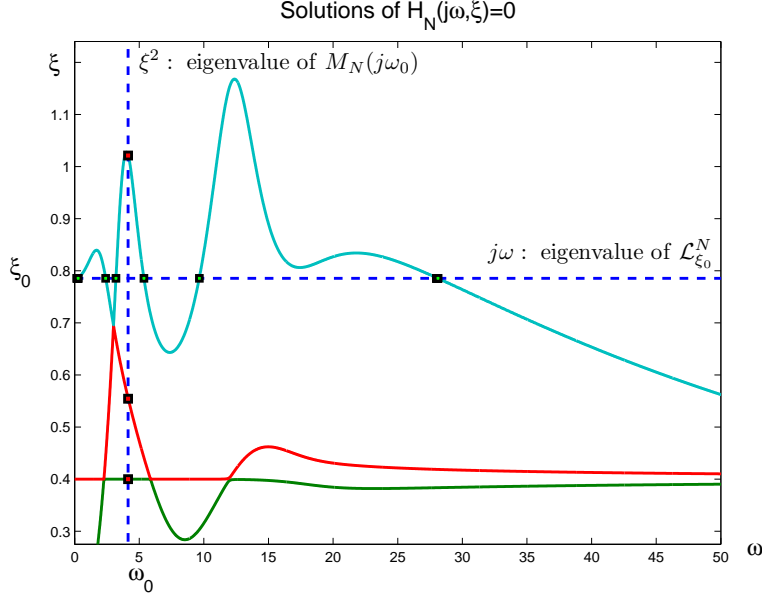


FIG. 3.1. Solutions of the equation (3.11) with  $N=10$ , for the problem data (5.1).

can be found by computing the imaginary axis eigenvalues of the matrix  $\mathcal{L}_{\xi}^N$ . Similarly, the intersections with vertical lines ( $\omega$  fixed) can be found by computing the positive real eigenvalues of the matrix  $M_N(j\omega)$ . This is illustrated in Figure 3.1.

In the remainder of the section, we discuss some spectral properties of the matrix  $M_N(j\omega)$ , defined in (3.12).

**PROPOSITION 3.5.** *The following statements hold.*

1. *The eigenvalues of  $M_N(j\omega)$  are real or appear in complex conjugate pairs.*
2. *The matrix  $M_N(j\omega)$  has  $2n_u$  eigenvalues  $\lambda_k(M_N(j\omega))$ ,  $1 \leq k \leq 2n_u$ , satisfying*

$$\lim_{\omega \rightarrow \infty} \lambda_k(M_N(j\omega)) = (\sigma_l(D))^2 \text{ for some } l \in \{1, \dots, n_u\}.$$

3. *If  $r(\omega) \geq 0$ , or, equivalently,  $|p_N(-\tau_0, j\omega)| \leq 1$ , then the matrix  $M_N(j\omega)$  is Hermitian.*
4. *If  $\tau_0 = 0$  then*

$$M_N(j\omega) = \begin{bmatrix} G_N(j\omega)^* G_N(j\omega) & 0 \\ 0 & D^T D \end{bmatrix},$$

where

$$G_N(j\omega) := C \left( j\omega I - A_0 - \sum_{i=1}^m A_i p_N(-\tau_i; j\omega) \right)^{-1} B + D, \quad (3.13)$$

with  $p_N$  defined by (3.6).

**Proof.** The first assertion follows from

$$M_N(j\omega) = \begin{bmatrix} \text{sign}(r(\omega))I & 0 \\ 0 & I \end{bmatrix} M_N(j\omega)^* \begin{bmatrix} \text{sign}(r(\omega))I & 0 \\ 0 & I \end{bmatrix}.$$

The assertion is implied by

$$\lim_{\omega \rightarrow \infty} M_N(j\omega) = \begin{bmatrix} D^T D & 0 \\ 0 & D^T D \end{bmatrix}.$$

The third assertion is trivial. The fourth assertion is due to  $p_N(-\tau_0; j\omega) \equiv 1$  and  $r(\omega) \equiv 0$  if  $\tau_0 = 0$ .  $\square$

The fourth assertion of Proposition 3.5 is of particular interest, because it shows that under the condition  $\tau_0 = 0$  the curves defined by (3.11) can be interpreted as the singular value curves of a rational approximation  $G_N(j\omega)$  of  $G(j\omega)$ .

To conclude the section we summarize the relations between the eigenvalue problems defined in Sections 2-3 in Table 3.1.

	implicit two parameter problem	horizontal search (explicit in $\omega$ )	vertical search (explicit in $\xi$ )	corresponding $\mathcal{H}_\infty$ -problem
continuous (§2.3)	$\det H(j\omega, \xi) = 0$	$(j\omega I - \mathcal{L}_\xi)u = 0$	$(\xi^2 I - G(j\omega)^* G(j\omega))v = 0$	$\ G(j\omega)\ _{\mathcal{H}_\infty}$
discretized (§3.2)	$\det H_N(j\omega, \xi) = 0$	$(j\omega I - \mathcal{L}_\xi^N)x = 0$	$(\xi^2 I - M_N(j\omega))v = 0$	$\ G_N(j\omega)\ _{\mathcal{H}_\infty}$ if $\tau_0 = 0$

TABLE 3.1

Relations between  $\mathcal{L}_\xi$ ,  $H(j\omega, \xi)$  and  $\|G(j\omega)\|_{\mathcal{H}_\infty}$ , as well as their discrete counterparts. The latter are all induced by a spectral discretization of the operator  $\mathcal{L}_\xi$  into the matrix  $\mathcal{L}_\xi^N$ .

**4. Algorithm.** Similar to the algorithm for the computation of characteristic roots of time-delay systems implemented in the package DDE-BIFTOOL [9], we propose an algorithm for computing  $\mathcal{H}_\infty$  norms that relies on a two-step approach. In the first step, outlined in §4.1, we approximate (predict) the  $\mathcal{H}_\infty$  norm based on the discretization of the operator  $\mathcal{L}_\xi$  into the matrix  $\mathcal{L}_\xi^N$ . In the second step, outlined in §4.2, we correct the results based on the reformulation of the eigenvalue problem for  $\mathcal{L}_\xi$  as a nonlinear eigenvalue problem of finite dimension. In §4.3 we discuss the choice of the discretization stepsize in the prediction step.

Throughout this section we assume that the grid  $\Omega_N$ , employed in the discretization of  $\mathcal{L}_\xi$ , consists of Chebyshev extremal points in the discretization, that is,

$$\theta_{N,i} = \cos\left(\frac{(N-i)\pi}{2N}\right), \quad i = -N, \dots, N. \quad (4.1)$$

**4.1. Prediction of the  $\mathcal{H}_\infty$  norm.** Inspired by Corollary 2.4 a natural way to approximate  $\|G(j\omega)\|_{\mathcal{H}_\infty}$  consists of computing

$$g_{\max}(N) := \inf \left\{ \xi > \sigma_1(D^T D) : \text{matrix } \mathcal{L}_\xi^N \text{ has no imaginary axis eigenvalues} \right\}, \quad (4.2)$$

where  $N$  is fixed. The following properties lay the basis for the corresponding algorithms.

PROPOSITION 4.1. *If the condition*

$$|p_N(-\tau_0; j\omega)| \leq 1, \quad \forall \omega \geq 0. \quad (4.3)$$

*is satisfied, then the following statements hold.*

1. The quantity  $g_{\max}(N)$ , defined in (4.2), is finite.

2. The matrix  $\mathcal{L}_\xi^N$  has eigenvalues on the imaginary axis for all

$$\xi \in (\sigma_1(D), g_{\max}(N)]$$

and no eigenvalues on the imaginary axis for  $\xi > g_{\max}(N)$ .

3. The matrix  $M_N(j\omega)$  has  $2n_u$  real eigenvalues  $\lambda_k(M_N(j\omega))$ ,  $1 \leq k \leq 2n_u$ , for all  $\omega \geq 0$ , satisfying

$$\lim_{\omega \rightarrow \infty} \lambda_k(M_N(j\omega)) = (\sigma_l(D))^2 \text{ for some } l \in \{1, \dots, n_u\}.$$

Moreover, if  $\tau_0 = 0$ , then

$$g_{\max}(N) = \|G_N(j\omega)\|_{\mathcal{H}_\infty},$$

where  $G_N(j\omega)$  is defined in (3.13).

**Proof.** The proof directly follows from Proposition 3.5 and Theorem 3.4.  $\square$

Notice that the condition (4.3) is always satisfied if  $\tau_0 = 0$ , which implies  $p_N(-\tau_0; j\omega) \equiv$

1. If  $\tau_0 \neq 0$ , then it is also satisfied, by the choice (4.1) of the grid  $\Omega_N$ .

The definition (4.2) and the properties 1.-2. described in Proposition 4.1 naturally lead to a bisection algorithm on the parameter  $\xi$  to compute  $g_{\max}(N)$ , similar to the algorithm presented in [8]. However, based on the interpretations described in §3.2 and property 3. of Proposition 4.1, the efficiency can be improved by performing a criss-cross search in the two parameter space  $(\omega, \xi)$ , instead of a search in the parameter  $\xi$  only. More precisely, an adaptation of the algorithm presented in [6] results in (see also [7]):

ALGORITHM 4.2.

Input: system data,  $N$ , symmetric grid  $\Omega_N$  defined by (4.1), candidate critical frequency  $\omega_t$  if available,

tolerance tol

Output:  $g_{\max}(N)$

1. compute a lower bound  $\xi_l$  on  $g_{\max}(N)$ ,  
e.g.  $\xi_l = \max \left\{ \sigma_1(G(0)), \sigma_1(D), \text{tol}, \sqrt{\max(\lambda_1(M_N(j\omega_t)), 0)} \right\}$
2. repeat until break
  - 2.1 set  $\xi := \xi_l(1 + 2 \text{ tol})$
  - 2.2 compute the set of eigenvalues  $\mathcal{E}_\xi$  of the matrix  $\mathcal{L}_\xi^N$  on the positive imaginary axis,  
 $\mathcal{E}_\xi := \left\{ j\omega^{(1)}, j\omega^{(2)}, \dots \right\}$ , with  $0 \leq \omega^{(1)} < \omega^{(2)} < \dots$
  - 2.3 if  $\mathcal{E}_\xi = \emptyset$ , break  
else  
 $\mu^{(i)} := \sqrt{\omega^{(i)}\omega^{(i+1)}}$ ,  $i = 1, 2, \dots$

$$\text{set } \xi_l := \max_i \sqrt{\max(\lambda_1(M_N(j\mu^{(i)})), \sigma_1(D)^2)},$$

{result: estimate  $(\xi + \xi_l)/2$  for  $g_{\max}(N)$ }

The underlying idea is illustrated in Figure 4.1, where some steps of the algorithm are visualized.

Algorithm 4.2 relies on the evaluation of the matrix  $M_N(\lambda)$ , and, hence, on the evaluation of the functions

$$\lambda \mapsto p_N(\pm\tau_i; \lambda), \quad i = 0, \dots, m$$

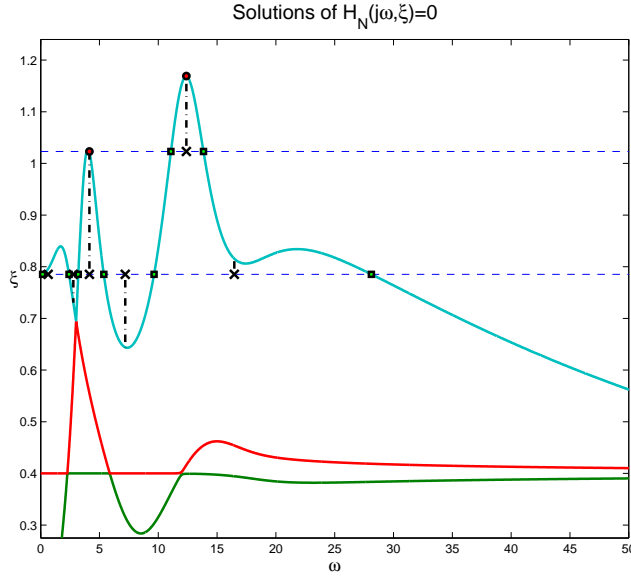


FIG. 4.1. *Some steps of Algorithm 4.2, for the problem data (5.1).*

for specific values of  $\lambda$ . For this, we represent  $p_N(\cdot; \lambda)$  in a polynomial basis:

$$p_N(t; \lambda) = \sum_{i=0}^{2N} \alpha_i T_i(t), \quad t \in [-1, 1],$$

where we suppress the dependence of the coefficients  $\alpha_i$  on  $\lambda$  in the notation. For  $\lambda \neq 0$ , the conditions (3.6) can be written as

$$(\lambda T - U) \begin{bmatrix} \alpha_0 \\ \vdots \\ \alpha_{2N} \end{bmatrix} = R, \quad (4.4)$$

where

$$T = \begin{bmatrix} T_0(\theta_{N,-N}) & \cdots & T_{2N}(\theta_{N,-N}) \\ \vdots & & \vdots \\ T_0(\theta_{N,-1}) & \cdots & T_{2N}(\theta_{N,-1}) \\ T_0(0) & \cdots & T_{2N}(0) \\ T_0(\theta_{N,1}) & \cdots & T_{2N}(\theta_{N,1}) \\ \vdots & & \vdots \\ T_0(\theta_{N,N}) & \cdots & T_{2N}(\theta_{N,N}) \end{bmatrix}, \quad U = \begin{bmatrix} T'_0(\theta_{N,-N}) & \cdots & T'_{2N}(\theta_{N,-N}) \\ \vdots & & \vdots \\ T'_0(\theta_{N,-1}) & \cdots & T'_{2N}(\theta_{N,-1}) \\ 0 & \cdots & 0 \\ T'_0(\theta_{N,1}) & \cdots & T'_{2N}(\theta_{N,1}) \\ \vdots & & \vdots \\ T'_0(\theta_{N,N}) & \cdots & T'_{2N}(\theta_{N,N}) \end{bmatrix}, \quad R = \begin{bmatrix} 0 \\ \vdots \\ 0 \\ \lambda \\ 0 \\ \vdots \\ 0 \end{bmatrix}.$$

The matrix  $T$  is always invertible, which can easily be deduced from a representation in a Lagrange basis. After solving (4.4) for a given value of  $\lambda$  we can evaluate

$$p_N(\pm\tau_i; \lambda) = \sum_{i=0}^{2N} \alpha_i T_i(\pm\tau_i), \quad i = 0, \dots, m.$$

Our implementation is based on a representation in an orthogonal basis of Chebyshev polynomials.

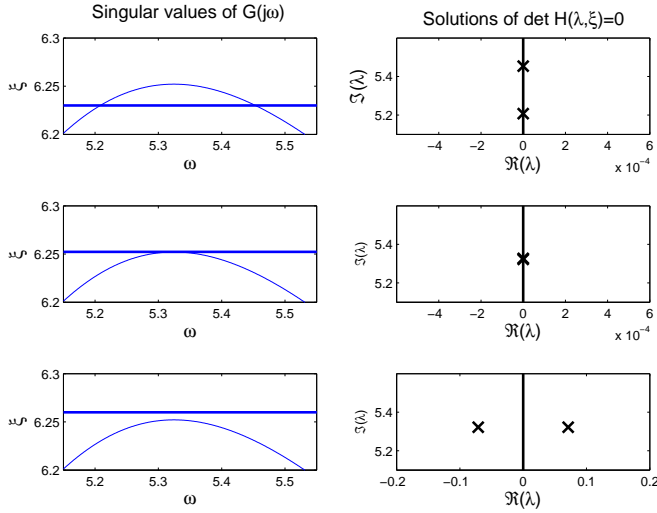


FIG. 4.2. (left) Intersections of the singular value plot of  $G$  with the horizontal line  $\xi = c$ , for  $c < \hat{\xi}$  (top),  $c = \hat{\xi}$  (middle) and  $c > \hat{\xi}$  (bottom). (right) Corresponding eigenvalues of the problem (2.4).

REMARK 4.3. We can formally write

$$p_N(t; \lambda) = S(t)(\lambda T - U)^{-1}R,$$

where  $S(t) = [T_0(t) \cdots T_{2N}(t)]$ . This shows that the functions  $p_N(\pm\tau_i; \lambda)$  are proper rational function of  $\lambda$ . Note that the coefficients of this rational function never need to be explicitly computed.

**4.2. Correction of the  $\mathcal{H}_\infty$  norm.** We describe how an approximation of  $\|G(j\omega)\|_{\mathcal{H}_\infty}$  can be corrected to the actual value. This is done by solving a set of nonlinear equations, which we derive first.

Let  $\hat{\xi} \geq 0$  and  $\hat{\omega} \geq 0$  are such that

$$\|G(j\omega)\|_{\mathcal{H}_\infty} = \hat{\xi} = \sigma_1(G(j\hat{\omega})), \quad (4.5)$$

and assume for the moment that the singular value  $\sigma_1(G(j\hat{\omega}))$  has multiplicity one. Then the nonlinear eigenvalue problem (2.4), with  $\xi = \hat{\xi}$ , has a double non-semisimple eigenvalue  $\lambda = j\hat{\omega}$  (see [11] for the definition of multiple eigenvalues of a nonlinear eigenvalue problem). This property is clarified in Figure 4.2. Therefore, setting

$$h(\lambda, \xi) = \det H(\lambda, \xi),$$

the pair  $(\hat{\omega}, \hat{\xi})$  satisfies

$$h(j\omega, \xi) = 0, \quad \frac{\partial h}{\partial \lambda}(j\omega, \xi) = 0. \quad (4.6)$$

These complex valued equations seem over-determined but this is not the case due to the spectral properties of the operator  $\mathcal{L}_\xi$ . As a corollary of Proposition 2.7 we namely get:

COROLLARY 4.4. For  $\omega \geq 0$ , we have

$$\Im h(j\omega, \xi) = 0 \quad (4.7)$$

and

$$\Re \frac{\partial h}{\partial \lambda}(j\omega, \xi) = 0. \quad (4.8)$$

**Proof.** From (2.10) we get

$$h(\lambda, \xi) = h(-\lambda, \xi), \quad \frac{\partial h}{\partial \lambda}(\lambda, \xi) = -\frac{\partial h}{\partial \lambda}(-\lambda, \xi).$$

Substituting  $\lambda = j\omega$  yields

$$\begin{aligned} h(j\omega, \xi) &= h(-j\omega, \xi) = (h(j\omega, \xi))^*, \\ \frac{\partial h}{\partial \lambda}(j\omega, \xi) &= -\frac{\partial h}{\partial \lambda}(-j\omega, \xi) = -\left(\frac{\partial h}{\partial \lambda}(j\omega, \xi)\right)^* \end{aligned}$$

and the assertions follow.  $\square$

Using Corollary 4.4 we can simplify the conditions (4.6) to

$$\begin{cases} \Re h(j\omega, \xi) = 0 \\ \Im \frac{\partial h}{\partial \lambda}(j\omega, \xi) = 0 \end{cases}. \quad (4.9)$$

In this way the pair  $(\hat{\omega}, \hat{\xi})$  satisfying (4.5) can be directly computed from the two equations (4.9), for example using Newton's method, provided that good starting values are available.

The drawback of working directly with (4.9) is that an explicit expression for the determinant of  $H(\lambda, \xi)$  is required. To avoid this, let  $v_1, v_2 \in \mathbb{C}^n$  be such that

$$H(j\omega, \xi) \begin{bmatrix} v_1 \\ v_2 \end{bmatrix} = 0, \quad n(v_1, v_2) = 0,$$

where  $n(v_1, v_2) = 0$  is a normalizing condition. Given the structure of  $H(j\omega, \xi)$  it can be verified that a corresponding left null vector is given by  $[-v_2^* \ v_1^*]$ . According to [11] a necessary condition for the eigenvalue  $\lambda = j\omega$  to be double but non-semisimple is given by<sup>1</sup>

$$[-v_2^* \ v_1^*] \frac{\partial H}{\partial \lambda}(j\omega, \xi) \begin{bmatrix} v_1 \\ v_2 \end{bmatrix} = 0. \quad (4.10)$$

A simple computation results in

$$[-v_2^* \ v_1^*] \frac{\partial H}{\partial \lambda}(j\omega, \xi) \begin{bmatrix} v_1 \\ v_2 \end{bmatrix} = 2\Im \left\{ v_2^* \left( I + \sum_{i=1}^p A_i \tau_i e^{-j\omega \tau_i} + BD_\xi^{-1} D^T C \tau_0 e^{j\omega \tau_0} \right) v_1 \right\}.$$

This expression is always real, which is a property inferred from (4.8). In this way we end up with  $4n + 3$  real equations

$$\begin{cases} H(j\omega, \xi) \begin{bmatrix} v_1 \\ v_2 \end{bmatrix} = 0 \\ n(v_1, v_2) = 0 \\ \Im \left\{ v_2^* \left( I + \sum_{i=1}^p A_i \tau_i e^{-j\omega \tau_i} + BD_\xi^{-1} D^T C \tau_0 e^{j\omega \tau_0} \right) v_1 \right\} = 0 \end{cases} \quad (4.11)$$

<sup>1</sup>The condition (4.10) guarantees the existence of a Jordan chain of length larger than one.



in the  $4n + 2$  unknowns  $\Re(v_1), \Im(v_1), \Re(v_2), \Im(v_2), \omega$  and  $\xi$ . These equations are still overdetermined because the property (4.7) is not explicitly exploited in the formulation, unlike the property (4.8). However, this property makes the equations (4.11) exactly solvable.

In our implementation we solve the equation (4.11) in least squares sense using the Gauss Newton algorithm, which can be shown to be quadratically converging in the case under consideration where the residual in the desired solution is zero. The program gives a warning when the correction involves a relative change larger than 10%, because this indicates that the approximation in the prediction step might not be accurate enough.

The above results can be used to compute the  $\mathcal{H}_\infty$  norm of  $G(j\omega)$ , in the following way. Given an approximation of a pair  $(\hat{\xi}, \hat{\omega})$  satisfying (4.5) and given corresponding estimates of  $v_1$  and  $v_2$ , we can find the exact values by solving the nonlinear equations (4.11) in least squares sense. The fact that the residual must be zero in the desired solution can be used as an additional optimality certificate. The approximation  $(\hat{\xi}, \hat{\omega})$  can be obtained by the prediction step outlined in §4.1. When using Algorithm 4.2 for the prediction step the total algorithm becomes:

ALGORITHM 4.5.

Input: system data,  $N$ , symmetric grid  $\Omega_N$  defined by (4.1), candidate critical frequency  $\omega_t$   
if available, tolerance  $\text{tol}$  for prediction step

Output:  $\|G(j\omega)\|_{\mathcal{H}_\infty}$

Prediction step:

*Apply Algorithm 4.2.*

Correction step:

1. determine all eigenvalues  $\{j\omega^{(1)}, \dots, j\omega^{(p)}\}$  of  $\mathcal{L}_{\xi_t}^N$  on the positive imaginary axis,
2. for all  $i \in \{1, \dots, p\}$ , solve (4.11) with starting values

$$\omega = \omega^{(i)}, \quad \xi = \xi_t, \quad \begin{bmatrix} v_1 \\ v_2 \end{bmatrix} = \arg \min \|H(j\omega^{(i)}, \xi_t)v\|/\|v\|;$$

denote the solution with  $(\tilde{u}^{(i)}, \tilde{v}^{(i)}, \tilde{\omega}^{(i)}, \tilde{\xi}^{(i)})$

3. set  $\|G(j\omega)\|_{\mathcal{H}_\infty} := \max_{1 \leq i \leq p} \tilde{\xi}^{(i)}$

**4.3. Number of discretization points.** An important aspect in the application of Algorithm 4.5 consists of choosing  $N$ , or, equivalently, the number of grid points for the discretization of  $\mathcal{L}_\xi$  into  $\mathcal{L}_\xi^N$ . On the one hand, from a computational point of view,  $N$  should be as small as possible, given that the computational cost of Algorithm 4.5 is dominated by the computation of the eigenvalues of the matrix  $\mathcal{L}_\xi^N$  with dimensions  $(2N + 1)2n$ . On the other hand,  $N$  should be sufficiently large to generate starting values for which the corrector converges to the desired values. In other but similar problems, in particular the problem of the computation of characteristic roots, mostly a heuristic or a 'safe' overestimate for the number of discretization points is used. In our case, the relations established in Sections 2-3 and summarized in Table 3.1 turn out to be very useful in the determination of  $N$ . This is explained in what follows.

From Definition 3.6 the function

$$t \in [-1, 1] \mapsto p_N(t; \lambda) \tag{4.12}$$

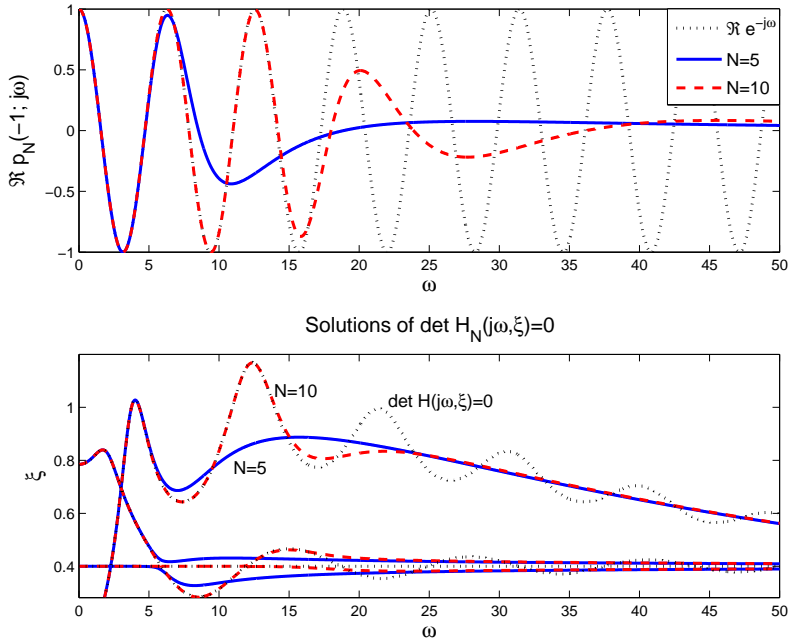


FIG. 4.3. (top) Comparison between the functions  $\omega \mapsto \exp(j\omega)$  and  $\omega \mapsto p_N(-1; j\omega)$  for  $N = 5$  and  $N = 10$ . (bottom) Corresponding comparison between the solutions of  $\det H(j\omega, \xi) = 0$  (the singular value plot of  $G$ ) and the solutions of  $\det H_N(j\omega; \xi) = 0$ , with problem data (5.1). An approximation with  $N = 10$  is sufficient to cover the highest peak, unlike an approximation with  $N = 5$ .

is an approximation of the function

$$t \in [-1, 1] \mapsto e^{\lambda t}. \quad (4.13)$$

Moreover, a comparison between  $H(\xi, \lambda)$ , defined by (2.2), and  $H_N(\xi, \lambda)$ , defined by (3.7), learns that the effect of approximating  $\mathcal{L}_\xi$  with  $\mathcal{L}_\xi^N$  can be interpreted as the effect of approximating the exponential functions  $e^{\pm\lambda\tau_i}$  with the rational functions  $p_N(\pm\tau_i; \lambda)$  for  $i = 0, \dots, m$ . Hence, the number  $N$  in the prediction step of Algorithm 4.5 should be chosen in such a way that

$$p_N(\pm\tau_i; j\omega) \approx e^{\pm j\omega\tau_i}, \quad i = 0, \dots, m,$$

in the relevant frequency range, that is, where the highest peak values in the singular value plot of  $G(j\omega)$  occur. This is illustrated in Figure 4.3.

In Figure 4.4 we depict the 'cut-off frequency'

$$\omega_c^\delta(N) := \min \left\{ \omega \geq 0 : \max_{t \in [-1, 1]} |e^{j\omega t} - p_N(t; j\omega)| \geq \delta \right\} \quad (4.14)$$

as a function of  $N$  for different values of  $\delta$ . The importance is as follows: if  $\omega \in [0, \omega_c^\delta(N)]$ , then it is guaranteed that  $p_N(\pm\tau_i; j\omega)$  approximates  $e^{\pm j\omega\tau_i}$  with relative error smaller than  $\delta$ , for  $i = 0, \dots, m$ . Because  $\omega_c^\delta$  is independent of the problem,

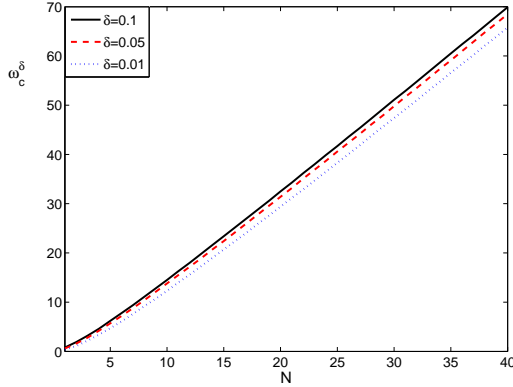


FIG. 4.4. The cut-off frequency  $\omega_c^\delta$ , as a function of  $N$ , for  $\delta = 0.01$ ,  $\delta = 0.05$  and  $\delta = 0.10$ .

Figure 4.4 can assist in determining a suitable value of  $N$ , when information about the relevant frequency range in the singular value plot of  $G$  is available. It is not necessary to choose  $\delta$  very small, because the prediction step in Algorithm 4.2 is followed by a correction step, hence, it is in the first place sufficient to capture qualitatively the highest peaks in the singular value plot. In our implementation of Algorithm 4.5 the value  $\delta = 0.1$  is taken. The user has the option to specify the corresponding cut-off frequency  $\omega_c^{0.1}$ , from which the value of  $N$  is automatically determined. Otherwise the default value  $N = 15$  is used. If in the prediction step a peak value is computed at a frequency  $\omega_p$  satisfying  $\omega_p > \omega_c^{0.1}$ , then a warning is generated with an advice to increase the cut-off frequency.

Our experience from extensive benchmarking learns that in most practical problems a very small value of  $N$  can be taken (the default  $N = 15$  is largely sufficient). This can be motivated as follows. First, via Corollary 2.4 the  $\mathcal{H}_\infty$  problem is transformed into a problem of checking the eigenvalues of  $\mathcal{L}_\xi$  on the imaginary axis. Because these eigenvalues are typically among the *smallest* eigenvalues of  $\mathcal{L}_\xi$  and the individual eigenvalues of  $\mathcal{L}_\xi^N$  exhibit *spectral convergence* to the corresponding eigenvalues of  $\mathcal{L}_\xi$  (this can be shown following the lines of [5]), a small value of  $N$  already yields good approximations of the imaginary axis eigenvalues. Second, in most applications the delay parameters are critical from a stability point of view, in the sense that increasing the delay parameters eventually destabilizes the system, but stability is maintained by decreasing the delay parameters (often referred to in the literature with the term delay-dependent stability). The connection between delay-dependent stability and the possibility to work with a small value of  $N$  in the  $\mathcal{H}_\infty$  computation is intuitively explained with an example.

EXAMPLE 4.6. We consider the transfer function

$$G(j\omega) = C(j\omega I - A_0 - A_1 e^{-j\omega\tau})^{-1} B + D,$$

with nominal delay  $\tau = \tau_n = 1$ . We assume that the system

$$\dot{x}(t) = A_0 x(t) + A_1 x(t - \tau) \quad (4.15)$$

is stable for all  $\tau \in [0, 1]$  but not delay-independent stable. It is well known that, if the delay is increased, characteristic roots can only cross the imaginary axis at a finite

number of points, say  $\{j\Omega_1, j\Omega_2, \dots\}$  (see e.g. [13]). The periodicity of the presence of an eigenvalue at  $j\Omega_i$  with respect to delay shifts of  $2\pi/\Omega_i$ , implies

$$\tau_n = 1 \leq \frac{2\pi}{\max_i \Omega_i}, \quad (4.16)$$

which leads to

$$1 \geq \frac{\max_i \Omega_i}{2\pi}.$$

If we choose  $N = 8$ , then we find from Figure 4.4 that  $\omega_c^{0.1} > 10$ . As a consequence, we get

$$\omega_c^{0.1} > 10 \geq \frac{10}{2\pi} \max_i \Omega_i \approx 1.59 \max_i \Omega_i.$$

This is expected to be sufficient for a correct computation of the  $\mathcal{H}_\infty$  norm of  $G$  because the highest peak values in the singular value plot of (4.15) typically occur in the frequency range where characteristic roots can come close to or cross the imaginary axis. Moreover, the factor 1.59 does not take into account the conservatism of the estimate (4.16), which can be very large.

**5. Numerical examples.** Throughout the paper, the obtained results and the ideas behind Algorithm 4.5 have been illustrated with the problem data

$$\begin{aligned} A_0 &= \begin{bmatrix} 108 & 110 & 18 \\ -107 & -109 & -17 \\ -217 & -217 & -37 \end{bmatrix}, A_1 = \begin{bmatrix} 46.5 & 46.5 & 1.5 \\ -46.5 & -46.5 & -1.5 \\ -93 & -93 & -3 \end{bmatrix}, \\ A_2 &= \begin{bmatrix} -0.3 & 0.3 & -0.3 \\ 0.3 & -0.3 & 0.3 \\ 0 & 0 & 0 \end{bmatrix}, B = \begin{bmatrix} 0.5 & -90 \\ -0.5 & 90 \\ 0 & 180 \end{bmatrix}, \\ C &= \begin{bmatrix} 1 & -1 & 1 \\ 0.1833 & 0.1833 & 0.1833 \end{bmatrix}, D = \begin{bmatrix} 0.4 & 0 \\ 0 & 0 \end{bmatrix}, \\ \tau_0 &= 0.5, \quad \tau_1 = 0.667, \quad \tau_2 = 1. \end{aligned}$$

In particular, the singular value plot of the corresponding transfer function  $G$  is shown in Figure 2.1 and the solutions of  $\det H_N(j\omega, \xi) = 0$  in Figure 3.1, for  $N = 10$ . The two parameter search in the prediction step is illustrated in Figure 4.1. The effect of the approximation in the prediction step is shown in Figure 4.3. With  $N = 10$ , the predicted  $\mathcal{H}_\infty$  norm is  $\xi_{pred} = 1.1626$  and the corrected  $\mathcal{H}_\infty$  norm is given by  $\xi_{corr} = 1.1696$ .

In Table 5.1 we present the results of benchmarking of our code with 12 problems. The second column shows the size of matrices  $A_i$ ,  $n$ , and the number of state delays,  $m$ . The third column gives the minimum value of  $N$  such that in the correction step the desired solution is computed. The fourth and fifth columns contain the predicted and corrected  $\mathcal{H}_\infty$  norms of the corresponding time-delay system. The plant  $G_{12}$  correspond to the problem data (5.1).

For the plant  $G_{12}$  a warning is generating when using the default value  $N = 15$ , indicating that the corresponding cut-off frequency might be too small. With  $N = 18$  no warning is given and the results are correct. We note that this example has been constructed in such a way that a relatively large value of  $N$  is necessary, by taking

Plants	$(n, m)$	$N$	$\xi_{pred}$	$\xi_{corr} (\ G(j\omega)\ _{\mathcal{H}_\infty})$
$G1$	(3, 1)	1	10.0235	10.0235
$G2$	(3, 1)	3	3.3693	3.3709
$G3$	(1, 1)	2	0.7158	0.7196
$G4$	(1, 1)	3	1.9230	1.9883
$G5$	(3, 3)	2	0.8852	0.8848
$G6$	(3, 3)	5	0.8974	0.9356
$G7$	(4, 3)	10	1.6259	1.6283
$G8$	(10, 7)	4	22.2979	22.3195
$G9$	(20, 9)	13	1.2827	1.2903
$G10$	(40, 3)	3	811.0898	814.6221
$G11$	(3, 2)	9	1.1579	1.1696
$G12^*$	(3, 2)	18	1.1626	1.1696

TABLE 5.1

Benchmarks for the  $\mathcal{H}_\infty$  norm computation.

very large values of 'non-critical' delay parameters (see the discussion on critical delay parameters in the paragraph before Example 4.6). When the delay parameters are critical from a stability point of view, which is the case in most practical problems, a much smaller values of  $N$  is sufficient, as motivated with Example 4.6.

The problem data for the above benchmark examples and a MATLAB implementation of our code for the  $\mathcal{H}_\infty$  norm computation are available at the website <http://www.cs.kuleuven.be/~wimm/software/hinf/>

**6. Discussion of alternative approaches and concluding remarks.** In this article we have described an algorithm for the computation of  $\mathcal{H}_\infty$  norms for time-delay systems, which relies on a two-step approach: a prediction step where an approximation is computed based on a finite-dimensional approximation, and a local corrector. It should be noticed that these two steps are to some extent independent of each other. In particular, other choices for a finite-dimensional approximation in the prediction step are possible. While our approach is based on a discretization of  $\mathcal{L}_\xi$  it is for instance also possible to use a direct approximation of the transfer function  $G$ , by replacing the exponential functions with a rational approximation. In this context our choice for a spectral discretization of  $\mathcal{L}_\xi$  is motivated as follows.

- An approach based on a spectral discretization of an appropriately defined derivative operator with nonlocal boundary conditions is known to be not only an accurate (cf. spectral convergence of the eigenvalues) but also a numerically stable way to solve infinite-dimensional eigenvalue problems in the context of time-delay system (see [5], see also [15] for a discussion on various methods for the "dual" problem of computing characteristic roots). On the contrary, working with an explicit rational approximation of  $G$  may lead to an ill-conditioned Hamiltonian matrix when applying Proposition 1.1 to the resulting finite-dimensional system. This is due to potential large differences in magnitudes of the coefficients in rational approximants of high order (a high order is necessary for "globally" capturing the transfer function in the relevant frequency range).
- From Definition 3.1 and Property 3.2 the effect of discretizing  $\mathcal{L}_\xi$  can be interpreted as the effect of approximating  $e^{\pm\lambda\tau_i}$  in  $H(\lambda, \xi)$  by  $p_N(\pm\tau_i; \lambda)$ , where the function (4.12) is obtained as a polynomial approximation of (4.13),

satisfying collocation and interpolation conditions on the grid  $\Omega_N$ , i.e. the exponential function is approximated over the full interval  $[-1 \ 1]$ , to which all delays belong. As a consequence, the dimensions of the matrix  $\mathcal{L}_\xi^N$ ,  $(2N + 1)2n \times (2N + 1)2n$ , are *independent* of the number of delays in the problem,  $m$ . This can also be seen from Remark 4.3, which shows that the poles of the rational functions  $\lambda \mapsto p_N(-\tau_i; \lambda)$  are independent of  $\tau_i$ , that is, one can interpret the effect of discretizing  $\mathcal{L}_\xi$  as the effect of an approximation of all exponential functions by rational functions with common poles. With Padé and many other types of rational approximations these poles are not the same, and the dimension of the discretized systems will become proportional to the number of delays.

- An important advantage of a direct rational approximation of the exponential functions in (1.1) is that a high accuracy in a relevant frequency range can easily be guaranteed by the choice of the order of the approximation. We have demonstrated that this is also possible when working with a spectral discretization of the operator  $\mathcal{L}_\xi$ , once again via the interpretation of the effect of its discretization as the effect of a rational approximation (although the coefficients of the rational functions  $p_N(-\tau_i; \lambda)$  never needed to be explicitly computed). This property was used in §4.3 for the determination of the number of discretization points.

The algorithm has been intensively tested, and turns out to be very robust. The computational cost is dominated by the determination of the eigenvalues of the matrix  $\mathcal{L}_\xi$ . In our current implementation all eigenvalues are computed. However, since the algorithm only needs the eigenvalues of  $\mathcal{L}_\xi$  in the vicinity of the imaginary axis, which are typically among the smallest eigenvalues, subspace methods based on inverse iteration become appealing for large problems. Instrumental to this the techniques described in Section 2.2 of [15] allow to bring the eigenvalue problem of  $\mathcal{L}_\xi$  in a form for which matrix vector become cheap. These issues, as well as the application of the algorithm to  $\mathcal{H}_\infty$  synthesis problems, are outside the scope of this paper.

**Acknowledgements.** This article present results of the Belgian Programme on Interuniversity Poles of Attraction, initiated by the Belgian State, Prime Ministers Office for Science, Technology and Culture, and of the Optimization in Engineering Centre OPTEC. The authors wish to thank the editors and anonymous reviewers for their careful reading and their constructive comments to improve the quality and readability of the paper.

#### REFERENCES

- [1] S. Boyd and V. Balakrishnan. A regularity result for the singular values of a transfer matrix and a quadratically convergent algorithm for computing its  $\mathcal{L}_\infty$ -norm. *Systems & Control Letters*, 15:1–7, 1990.
- [2] S. Boyd, V. Balakrishnan, and P. Kabamba. A bisection method for computing the  $\mathcal{H}_\infty$  norm of a transfer matrix and related problems. *Mathematics of Control, Signals and Systems*, 2:207–219, 1989.
- [3] D. Breda, S. Maset, and R. Vermiglio. Computing the characteristic roots for delay differential equations. *IMA Journal of Numerical Analysis*, 24:1–19, 2004.
- [4] D. Breda, S. Maset, and R. Vermiglio. Pseudospectral differencing methods for characteristic roots of delay differential equations. *SIAM Journal on Scientific Computing*, 27(2):482–495, 2005.
- [5] D. Breda, S. Maset, and R. Vermiglio. Pseudospectral approximation of eigenvalues of derivative operators with non-local boundary conditions. *Applied Numerical Mathematics*, 56:318–331, 2006.

- [6] N.A. Bruinsma and M. Steinbuch. A fast algorithm to compute the  $\mathcal{H}_\infty$ -norm of a transfer function matrix. *Systems and Control Letters*, 14:287–293, 1990.
- [7] J.V. Burke, A.S. Lewis, and M.L. Overton. Robust stability and a criss-cross algorithm for pseudospectra. *IMA Journal of Numerical Analysis*, 23:359–375, 2003.
- [8] R. Byers. A bisection method for measuring the distance of a stable matrix to the unstable matrices. *SIAM Journal on Scientific and Statistical Computing*, 9(9):875–881, 1988.
- [9] K. Engelborghs, T. Luzyanina, and G. Samaey. DDE-BIFTOOL v. 2.00: a Matlab package for bifurcation analysis of delay differential equations. TW Report 330, Department of Computer Science, Katholieke Universiteit Leuven, Belgium, October 2001.
- [10] Y. Genin, R. Stefan, and P. Van Dooren. Real and complex stability radii of polynomial matrices. *Linear Algebra and its Applications*, 351-352:381–410, 2002.
- [11] R. Hryniv and P. Lancaster. On the perturbation of analytic matrix functions. *Integral Equations and Operator Theory*, 34:325–338, 1999.
- [12] W. Michiels, E. Fridman, and S.-I. Niculescu. *Robustness assessment via stability radii in delay parameters*. International Journal of Robust and Nonlinear Control, 2009. In press (published on-line).
- [13] W. Michiels and S.-I. Niculescu. *Stability and stabilization of time-delay systems. An eigenvalue based approach*. SIAM, 2007.
- [14] Trefethen. *Spectral methods in MATLAB*, volume 10 of *Software, Environments, and Tools*. SIAM, 2000.
- [15] K. Verheyden. *Numerical bifurcation analysis of large-scale delay differential equations*. PhD thesis, Department of Computer Science, K.U.Leuven, 2007.
- [16] K. Zhou, J.C. Doyle, and K. Glover. *Robust and optimal control*. Prentice Hall, 1995.